The Co-seismic Ionospheric Disturbance during 2023 Mw7.8 and Mw7.5 Turkey Double Earthquake Monitored by GNSS Observations

Wei Li *, Keke Wang, Yongxin Chen and Guangxing Wang

China University of Geosciences, Wuhan, China

* weili@cug.edu.cn

Abstract

Turkey experienced double strong earthquakes on 6 February 2023 at UTC 01:17:34 with a magnitude of 7.8 and UTC 10:24:50 with a magnitude of 7.5. The propagation direction of the ionospheric disturbances are coincide with the rupture zones, the north-eastern and south-western bi-directional ruptures, and the east-west ruptures. According the result of Turkey station, it is found that the CIDs of the first earthquake are mainly caused by acoustic, but also by Rayleigh wave and mixed wave. Due to the influence of the first earthquake and aftershocks, the CIDs of the second earthquake are dominated by mixed waves. The CID of Japan in the first earthquake was caused by gravity wave and Rayleigh wave, and the second earthquake was mainly caused by Rayleigh wave. The amplitude of the ionospheric disturbance caused by the Mw7.5 earthquake in Turkey is stronger than that of the Mw7.8 earthquake, while the area of the disturbance caused by the Mw7.8 earthquake is larger than that of the Mw7.5 earthquake. Meanwhile, confirmed that significant CIDs will be detected when strike-slip earthquake magnitude is large enough..

Introduction

During earthquakes, the generation of sub-pressure waves in the atmosphere leads to their coupling with the ionosphere, resulting in variations in electron density. This phenomenon is referred to as Co-seismic Ionospheric Disturbances (CIDs). The advancement of space geodesy technology has revolutionized monitoring methods by overcoming the limitations of traditional approaches. GNSS (Global Navigation Satellite System), known for its exceptional accuracy, unrestricted temporal and spatial capabilities, and easy accessibility, has played a pivotal role in this breakthrough. GNSS observations can deduce global ionospheric variation characteristics, thus effectively addressing the scarcity of earthquake near-field data. Furthermore, they provide reliable data support for analyzing the propagation characteristics of energy released by earthquakes through ionospheric variations. Multiple studies have consistently demonstrated that detectable CIDs occur in earthquakes of magnitude Mw>6.5. The current study of CIDs mainly focuses on single earthquakes and lacks a comprehensive investigation of the time domain, frequency domain, and spatial characteristics. On February 6, 2023, a powerful earthquake with a magnitude of 7.8 struck Turkey at UTC 1:17, which occurred at the confluence of the Anatolian Plate, the Arabian Plate, and the African Plate. And then less than nine hours later, a magnitude 7.5 earthquake occurred again, almost 96 kilometers away from the previous one. The two earthquakes formed a rare " double-shock" earthquake sequence in history, and later induced a series of strong aftershocks, forming a swarm-type earthquake. As a result, this study plans to analyze the CIDs caused by the doublet, by extracting ionospheric TEC from GNSS data obtained from Turkey area and Japan area. By using the Butterworth Filter to process the disturbance sequences, the study analyzes the change characteristics of CIDs in the time domain, the spatial propagation direction, and propagation velocity. Then, the short-time Fourier transformation is applied to perform spectral analysis. By performing a comprehensive analysis, the study aims to determine the type of seismic waves causing CIDs, understand the impact range and propagation mode, and evaluate the ionospheric changes caused by the Turkey earthquake.

Methodology

By using the dual frequency observations obtained from GNSS, the STEC value at the ionospheric puncture point (IPP) on the radio propagation path can be obtained, and then the precise VTEC value at the IPP can be obtained through differential code deviation (DCB) and mapping function. This article mainly uses carrier phase observations to smooth pseudorange observations and extract TEC.

$$D_1 = P_1 - \frac{40.3}{f_1^2}\int_s N_e ds \qquad D_2 = P_2 - \frac{40.3}{f_2^2}\int_s N_e ds$$

$$\Delta P = P_1 - P_2 = 40.3\left(\frac{1}{f_1^2} - \frac{1}{f_2^2}\right)\int_s N_e ds \qquad TEC_P = \int_s N_e ds = -\frac{1}{40.3}\frac{f_1^2 f_2^2}{f_1^2 - f_2^2}\Delta P$$

$$D_1 = c\frac{\Phi_1 + 2\pi n_1}{f_1} + \frac{40.3}{f_1^2}\int_s N_e ds \qquad D_2 = c\frac{\Phi_2 + 2\pi n_2}{f_2} + \frac{40.3}{f_2^2}\int_s N_e ds$$

$$TEC_\Phi = \int_s N_e ds = \frac{c}{40.3}\frac{f_1^2 f_2^2}{f_1^2 - f_2^2}\left(\frac{\Phi_1}{f_1} - \frac{\Phi_2}{f_2}\right) + \Delta n$$

$$TEC = \frac{f_1^2 f_2^2}{40.3\left(f_1^2 - f_2^2\right)}\left(\widetilde{P_2} - \widetilde{P_1} + \Delta b_r + \Delta b_s\right)$$

$$VTEC = cos\left(arcsin\left(\frac{R}{R+H}sin(\alpha z)\right)\right)\left[-\frac{f_1^2 f_2^2}{40.3\left(f_1^2 - f_2^2\right)}\left(P_{4,sm} - cDCB_j - cDCB^i\right)\right]$$

Butterworth filter has the characteristic of the maximum flat frequency response in the passband without fluctuations and gradually decreases to zero in the stopband. Compared to the Chebyshev filter, the Savitzky-Golay sliding filter, etc., the Butterworth filter performs more smoothly, and no ripple phenomenon exists in the passband.

$$H(u,v) = \frac{\left[\frac{D(u,v)W}{D^2(U,V) - D_0^2}\right]^{2n}}{1 + \left[\frac{D(u,v)W}{D^2(U,V) - D_0^2}\right]^{2n}}$$

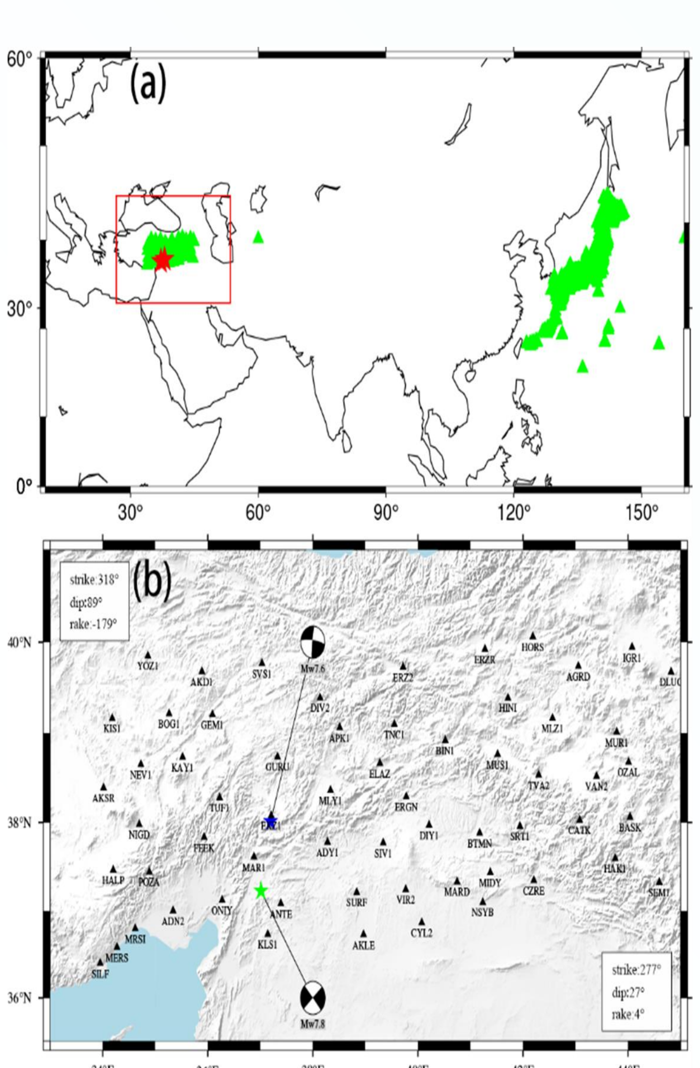

Results

62 GNSS observation stations around the earthquake provided by Türkiye officials were selected and 423 CORS observation stations in Japan to comprehensive analysis of GNSS observations.. Specifically, this study mainly focuses on ionospheric disturbances caused by direct sound waves generated in the near field during earthquakes which this kind of shock wave crosses the frequency branch of the acoustic mode, so a filter window of 2~8mHz is used to highlight the acoustic mode signal. And in the far field, in order to identify the atmosphere with low dispersion and long-distance transmission characteristics of gravitational wave signal, that is 0.3~2 mHz.

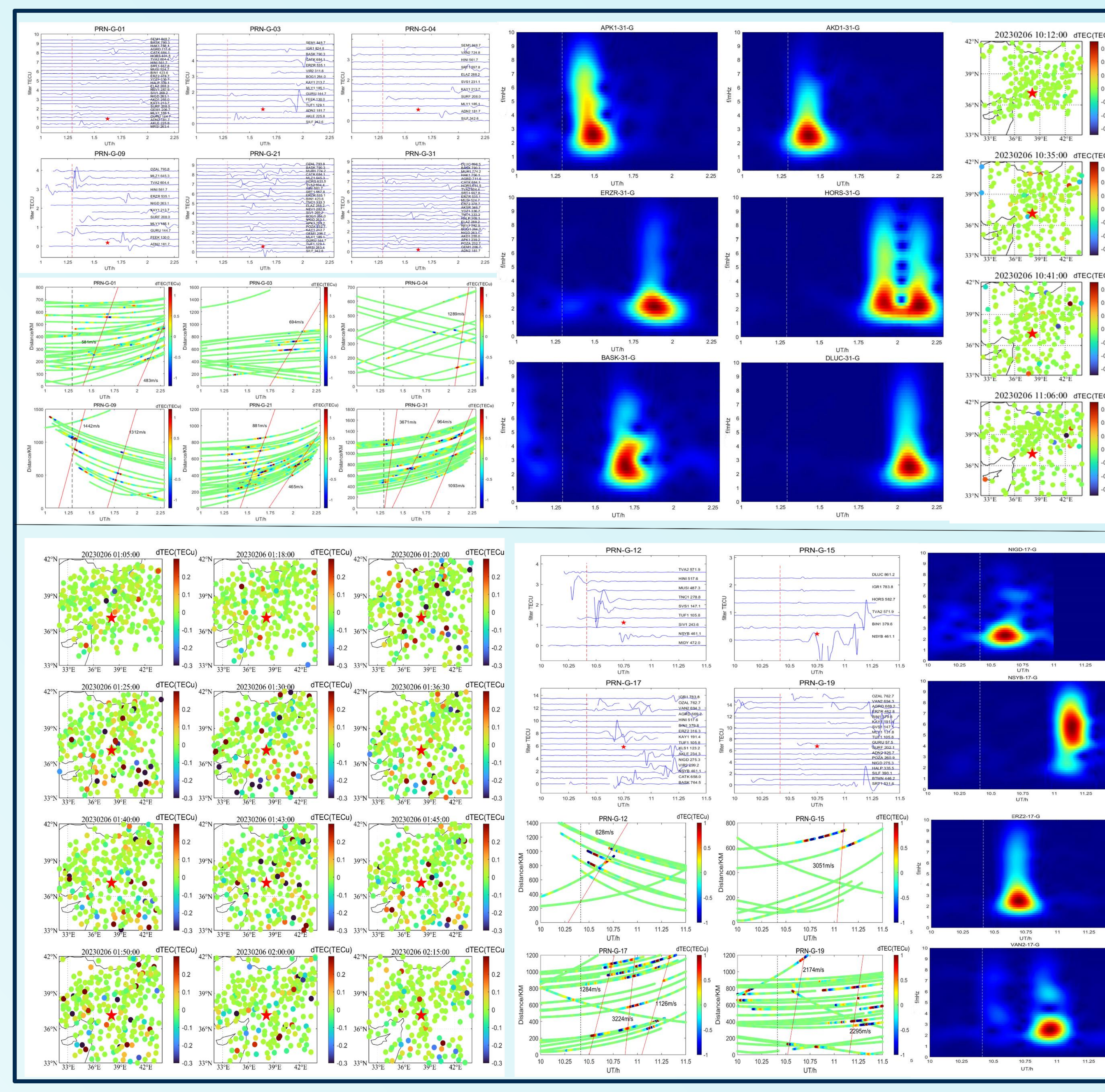

Spatial temporal characteristics of CIDs in Turkey area

Spatial-temporal characteristics of CIDs in Japan area

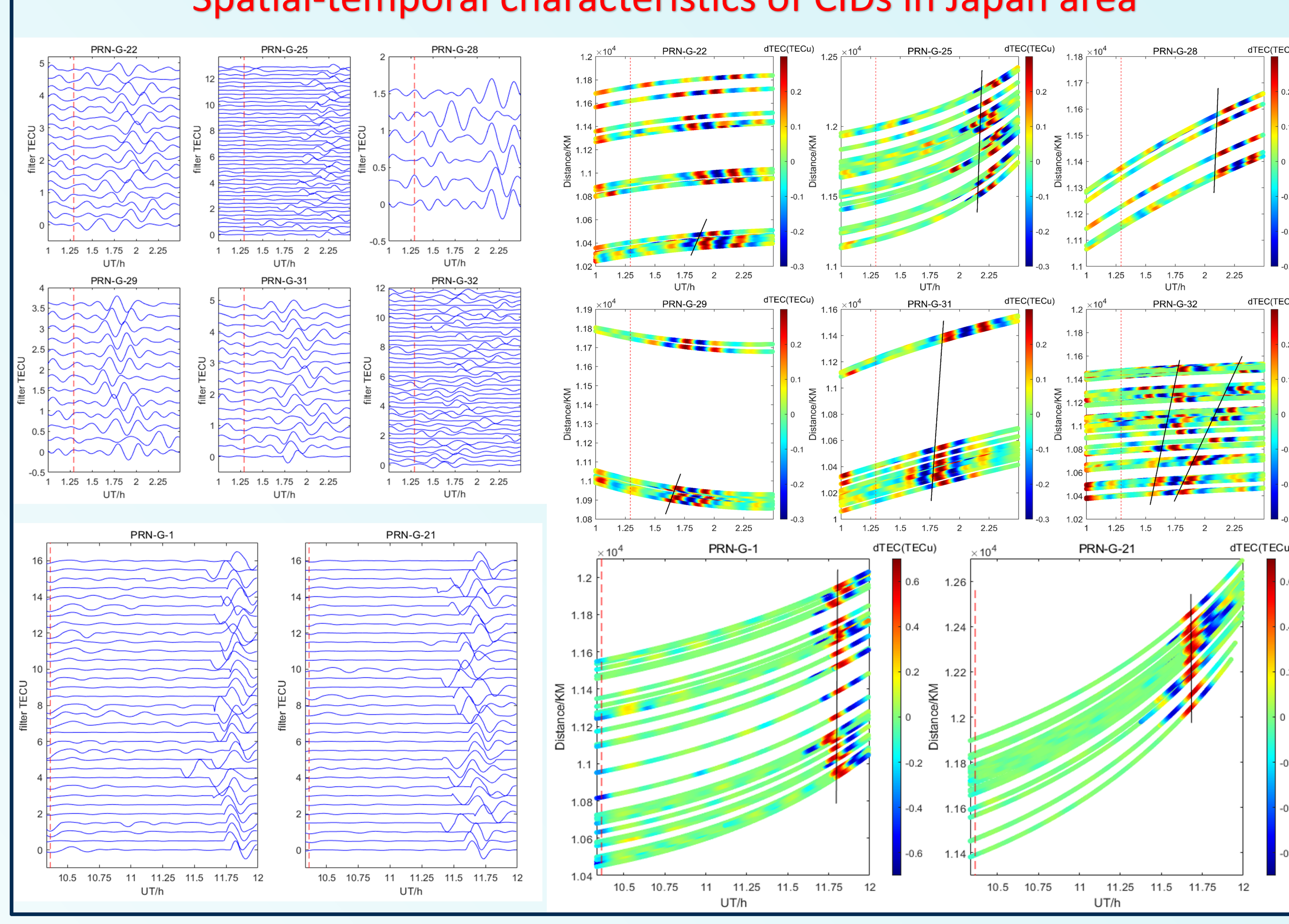

Conclusion

By qualitatively and quantitatively assessing the location, time, epicenter distance, and propagation velocity of the CIDs caused by the Turkey earthquake, we evaluate the progression of the CIDs and the post-seismic propagation characteristics. It is worth noting among the characterization results of CIDs propagation, the amplitude of the ionospheric disturbance caused by the Mw7.5 earthquake in Turkey is stronger than that of the Mw7.8 earthquake, while the area of the disturbance caused by the Mw7.8 earthquake is larger than that of the Mw7.5 earthquake. There are two possible reasons for this situation. First, according to the public data of seismometers, the interval between earthquake tremors during the first earthquake is shorter than that of the second earthquake. Second, its initial Turkey area and Japan area are in the night when the first earthquake strikes, the second earthquake time for the day, and the night of the ionosphere value lower than during the day. Meanwhile, Artem Vesnin et al. also proposed the third reason, namely the effect of neutral wind. the orientation and propagation direction of the ionospheric disturbances also coincide with the rupture zones of the two Turkey earthquakes, the north-eastern and south-western bi-directional ruptures, and the east-west ruptures. The results of the station in Turkey show that the CID induced during the first earthquake is mainly caused by sound wave, with a part of mixed wave and Rayleigh wave, wherein the mixed wave is a kind of hybrid superposition wave formed by the coupling of the acoustic wave caused by the earthquake and the propagating Rayleigh wave. The CIDs of the second earthquake are mainly caused by mixed waves, which may be because the seismic waves generated after the second earthquake are affect.